

Enhancement of Crystallinity in ZnO:Al Films Using a Two-Step Process Involving the Control of the Oxygen Pressure

Taeho Moon*, Wonki Yoon, Seung-Yoon Lee, Kwang Sun Ji,
Young-Joo Eo, Seh-Won Ahn, and Heon-Min Lee[†]

Devices and Materials Laboratory, LG Electronics, Seoul 137-724

(Received December 9, 2009, Revised February 9, 2010, Accepted February 10, 2010)

ZnO:Al films were deposited by DC-pulsed magnetron sputtering using a two-step process involving the control of the oxygen pressure. The seed layers were prepared with various Ar to oxygen flow ratios and the bulk layers were deposited under pure Ar. As the oxygen pressure during the deposition of the seed layer increased, the crystallinity and degree of (002) texturing increased. The resistivity gradually decreased with increasing crystallinity from $4.7 \times 10^{-4} \Omega \cdot \text{cm}$ (no seed) to $3.7 \times 10^{-4} \Omega \cdot \text{cm}$ (Ar/O₂ = 9/1). The etched surface showed a crater-like structure and an abrupt morphology change appeared as the crystallinity was increased. The sample deposited at an Ar/O₂ flow ratio of 9/1 showed a very high haze value of 88% at 500 nm, which was explained by the large feature size of the craters, as shown in the AFM image.

Keywords : ZnO:Al film, Transparent conductive oxide, Crystallinity, Si thin-film solar cell

Transparent conducting oxides (TCOs) have been used for a variety of optoelectric devices, such as flat panel displays and thin-film solar cells [1–3]. Among the various TCOs, ZnO:Al has been the object of significant research activities for Si thin-film solar cells, because of its easy texturing by wet-chemical etching and large feature size compared with that of SnO₂:F. Surface texturing extends the effective path length of the scattered light within the active Si layers, which can result in the minimization of the thickness of the Si layers, while maintaining the efficiency, leading to a decrease of the production cost [2]. Also, the large feature size of the surface texture results in high haze (diffused light/total-transmitted light), which increases the degree of light trapping

[3]. This etching behavior is very sensitive to the crystallinity of the as-deposited film [4]. In addition, one method of increasing the transparency while maintaining the resistivity is to improve the carrier mobility, due to free carrier absorption, and the carrier mobility can be improved by increasing the crystallinity [5].

There have been a few reports on the use of seed layers such as ZnS, Lu₂O₃, and SiC for improving the crystallinity of ZnO films, but these seed layers incur an additional process cost [6–8]. Recently, Kang *et al.* reported a two-step process involving the control of the oxygen flow, and a significant improvement in the degree of crystallinity was shown with the use of a seed layer [9]. However, there have been no studies

* [E-mail] taeho@lge.com

[†] [E-mail] hmlee@lge.com

in which the deposition conditions of the seed layer were examined. Herein, we report on the microstructural changes of ZnO:Al films as a function of the Ar to oxygen flow ratio during the deposition of the seed layer.

The ZnO:Al films were deposited on Corning 1737 glass by pulsed-DC magnetron sputtering using a ZnO:Al target with 2 wt.% Al₂O₃ at a deposition temperature of 320°C. To systematically examine the characteristics of the ZnO:Al films as a function of the deposition conditions of the seed layer, seed layers were prepared with various Ar to oxygen flow ratios ranging from 24/1 to 4/1 and the bulk layers were deposited under pure Ar. Also, a sample without a seed layer was prepared as a reference. The working pressure was fixed at 1.5 mTorr during all of the deposition steps. Surface texturing was performed by wet-chemical etching using dilute HCl acid (0.5%) at room temperature to investigate the light-scattering characteristics. The sheet resistances of etched films were adjusted to $5.2 \pm 0.2 \ \Omega/\square$ by changing the etching time.

The microstructure was analyzed by x-ray diffraction (XRD : D/MAX-IIIC, Rigaku). The four-point probe method was used to evaluate the sheet resistance and resistivity. The surface morphology was examined in a scan area of $10 \ \mu\text{m}^2$ by atomic force microscopy (AFM : Nanoscope IIIa, Digital Instrument). The transmittance was obtained in the range from 350 nm to 1100 nm by means of a spectrophotometer (Cary 5000, Varian) and the haze values were calculated with specula components and diffuse components. The thicknesses of the seed layer and bulk layer before etching were $\sim 80 \ \text{nm}$ and $\sim 1,300 \ \text{nm}$, respectively, as measured by a surface profiler.

The XRD patterns (in a log scale) of the ZnO:Al films with different Ar to O₂ flow ratios during the deposition of the seed layer are shown in Fig. 1. The sample without a seed layer shows (002) texturing with minor peaks of (101) and (103), and the extent of

(002) texturing increases with increasing oxygen pressure. (The peaks marked with an asterisk are the (002) diffractions due to Cu K_{β} radiation.) The slope of the Δk vs. k plot (the scattering vector, $k = (4\pi/\lambda) \text{Sin}\Theta$) shows a non-uniform distribution of the local strain ($\Delta d/d$) [10,11]. The two peaks of (002) and (004) were fitted using a Lorentzian function and the variation of the peak widths, Δk (full width at half maximum), with the Ar to O₂ flow ratio is shown in the inset of

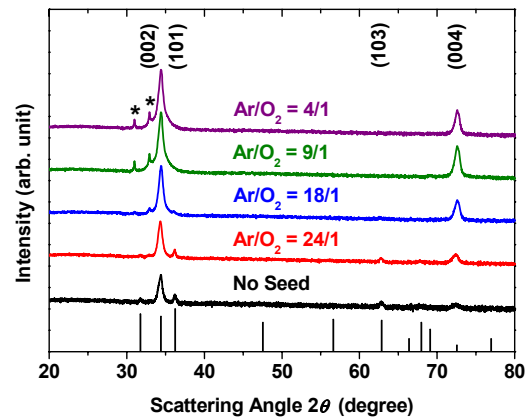


Figure 1. XRD patterns (on a log scale) of the ZnO:Al films with different Ar to O₂ flow ratios during the deposition of the seed layer. The ideal peak positions and intensities for hexagonal ZnO (JCPDS #36-1451) are marked at the bottom. (The peaks marked with an asterisk are the (002) diffractions due to Cu K_{β} radiation.)

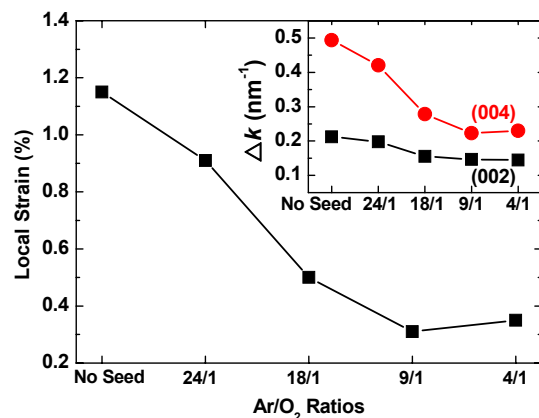


Figure 2. Local strains ($\Delta d/d$) of the ZnO:Al films with different Ar to O₂ flow ratios during the deposition of the seed layer. The inset shows the variation in the XRD peak widths, Δk (full width at half maximum), of the (002) and (004) diffractions.

Fig. 2. As the oxygen pressure increases, a decrease of the local strain (increase of crystallinity) is clearly shown (Fig. 2).

The resistivity of the ZnO:Al films as a function of the Ar to O₂ flow ratio during the deposition of the seed layer is shown in Fig. 3. The resistivities were calculated from the sheet resistance and bulk-layer thickness. (The seed layers deposited in the presence of oxygen flow were highly resistive. For example, the sheet resistance of the seed layer deposited under the conditions of Ar/O₂ = 9/1 was ~100 kΩ/□.) As the oxygen pressure increases, the resistivity gradually decreases from 4.7×10⁻⁴ Ω·cm (no seed) to 3.7×10⁻⁴ Ω·cm (Ar/O₂ = 9/1), which is well correlated with the change of crystallinity, as shown in Fig. 2.

The AFM images of the etched ZnO:Al films are shown in Fig. 4. The etched surfaces show a crater-like structure and an abrupt morphology change appears as the oxygen pressure is increased. Fig. 4(a), 4(b), and 4(c) show that the surface is uniformly covered by craters with a lateral size of ~1 μm. The root-mean-square (RMS) value of the surface roughness gradually increases with increasing oxygen pressure from 72 nm (no seed) to 100 nm (Ar/O₂ = 18/1). However, Fig. 4(d) shows a nonuniform surface morphology that consists of shallow craters and large craters with a

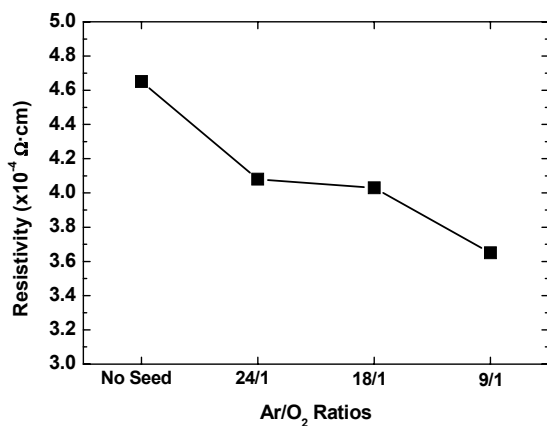


Figure 3. Resistivities of the ZnO:Al films with different Ar to O₂ flow ratios during the deposition of the seed layer.

lateral size of ~3 μm. Also, the surface roughness shows a high RMS value of 142 nm. Previously, the modified Thornton model was used to describe structural properties and surface morphology for sputter-deposited ZnO:Al films, and a film with high crystallinity was found to result in an irregular etching process [4]. Therefore, the abrupt change of the etching mode as the oxygen pressure was increased is likely due to the decrease in the number of chemical attack sites with increasing crystallinity, which may be explained by the drastic decrease in the number of structural defects, such as point-defect segregation in the grain boundary [12].

Fig. 5 shows the total transmittance and haze values of the etched ZnO:Al films. The sheet resistances of all of the films were adjusted to 5.2±0.2 Ω/□ by changing the etching time. The total transmittance increases with increasing oxygen pressure, which is explained by the change in the thickness caused by the difference of the resistivity. The effective thicknesses after etching (that is calculated from the resistivity before etching and the sheet resistance after etching) gradually decrease with increasing oxygen pressure from ~1.5

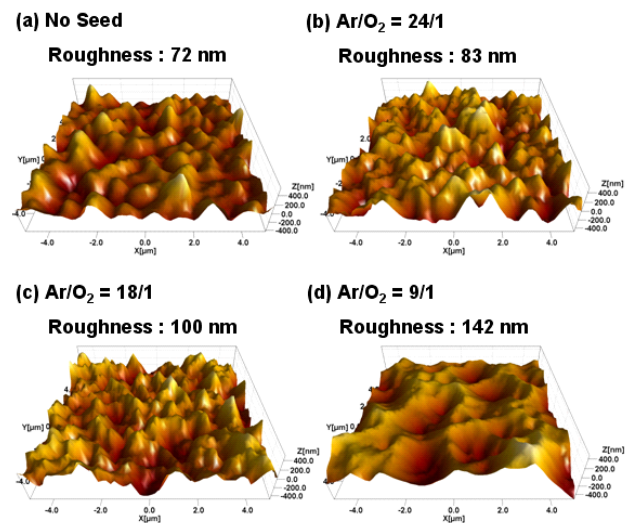


Figure 4. AFM images of the etched ZnO:Al films with different Ar to O₂ flow ratios during the deposition of the seed layer. The RMS values of the surface roughness increase with increasing oxygen pressure.

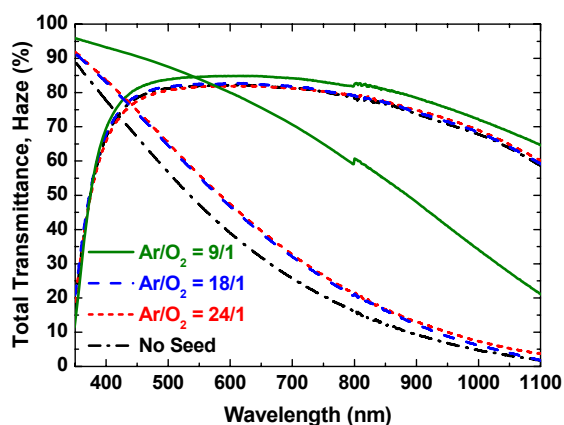


Figure 5. Total transmittance and haze (diffused/total transmitted) values of the etched ZnO:Al films with different Ar to O₂ flow ratios during the deposition of the seed layer. The sheet resistances of all of the films were adjusted to $5.2 \pm 0.2 \ \Omega / \square$ through the change of the etching time.

μm (no seed) to $\sim 1.1 \ \mu\text{m}$ ($\text{Ar}/\text{O}_2 = 9/1$). The haze values increase with increasing oxygen pressure. Especially, the sample deposited at a flow ratio of $\text{Ar}/\text{O}_2 = 9/1$ shows a very high haze value of 88% at 500 nm, which is explained by the large feature size of the craters, as shown in Fig. 4(d) [3].

In conclusion, ZnO:Al films were deposited by DC-pulsed magnetron sputtering using a two-step process involving the control of the oxygen pressure. The seed layers were prepared with various Ar to oxygen flow ratios ranging from 24/1 to 4/1 and the bulk layers were deposited under pure Ar. As the oxygen pressure increased, the crystallinity obtained from the Δk vs. k plots and the degree of (002) texturing increased. The resistivity gradually decreased with increasing crystallinity from $4.7 \times 10^{-4} \ \Omega \cdot \text{cm}$ (no seed) to $3.7 \times 10^{-4} \ \Omega \cdot \text{cm}$ ($\text{Ar}/\text{O}_2 = 9/1$). The etched surface showed a crater-like structure and an abrupt morphology change appeared as the crystallinity was increased. The RMS value of the surface roughness gradually increased with increasing oxygen pressure from 72 nm (no seed) to 142 nm ($\text{Ar}/\text{O}_2 = 9/1$). The sample prepared at a flow ratio of $\text{Ar}/\text{O}_2 = 9/1$ showed a very high haze value of 88% at 500 nm, which was explained

by the large feature size of the craters, as shown in the AFM image. Detailed studies are needed to clarify the exact mechanism underlying the change of the microstructure according to the deposition conditions of the seed layer and correlate this mechanism with the solar cell performance.

ACKNOWLEDGEMENTS

The authors are grateful to Young Il Jang and Seung Kyu Moon for the materials characterizations. This work was supported by the Korean Ministry of Knowledge Economy (2008NPV12J032100).

REFERENCES

- [1] T. Moon, G. Y. Hong, H.-C. Lee, E.-A. Moon, B. W. Jeung, S.-T. Hwang, J. S. Kim, and B.-G. Ryu, *Electrochem. Solid-State Lett.* **12**, J61 (2009).
- [2] J. Müller, B. Rech, J. Springer, and M. Vanecek, *Solar Energy* **77**, 917 (2004).
- [3] Y. Zhao, S. Miyajima, Y. Ide, A. Yamada, and M. Konagai, *Jpn. J. Appl. Phys.* **41**, 6417 (2002).
- [4] O. Kluth, G. Schöpe, J. Hüpkas, C. Agashe, J. Müller, and B. Rech, *Thin Solid Films* **442**, 80 (2003).
- [5] C. Agashe, O. Kluth, J. Hüpkas, U. Zastrow, B. Rech, and M. Wuttig, *J. Appl. Phys.* **95**, 1911 (2004).
- [6] T. Onuma, S. F. Chichibu, A. Uedono, Y.-Z. Yoo, T. Chikyow, T. Soda, M. Kawasaki, and H. Koinuma, *Appl. Phys. Lett.* **85**, 5586 (2004).
- [7] W. Guo, A. Allenic, Y. B. Chen, X. Q. Pan, W. Tian, C. Adamo, and D. G. Schlom, *Appl. Phys. Lett.* **92**, 072101 (2008).
- [8] Y. Zhang, H. Zheng, J. Su, B. Lin, and Z. Fu, *J. Lumin.* **124**, 252 (2007).
- [9] D.-W. Kang, S.-H. Kuk, K.-S. Ji, S.-W. Ahn, and

- M.-K. Han, Mater. Res. Soc. Symp. Proc. **1153**, A07-19 (2009).
- [10] T. Moon, B. Lee, T.-G. Kim, J. Oh, Y. W. Noh, S. Nam, and B. Park, Appl. Phys. Lett. **86**, 182904 (2005).
- [11] T. Moon, S.-T. Hwang, D.-R. Jung, D. Son, C. Kim, J. Kim, M. Kang, and B. Park, J. Phys. Chem. C **111**, 4164 (2007).
- [12] J. Owen, J. Hüpkes, and E. Bunte, Mater. Res. Soc. Symp. Proc. **1153**, A07-08 (2009).

산소 압력의 조절과 함께 두 번의 증착 과정을 이용한 ZnO:Al 박막에 결정성의 향상

문태호* · 윤원기 · 이승윤 · 지광선 · 어영주 · 안세원 · 이현민†

소자재료연구소, LG전자, 서울 137-724

(2009년 12월 9일 받음, 2010년 2월 9일 수정, 2010년 2월 10일 확정)

ZnO:Al 박막은 산소 압력을 조절한 두 번의 증착 과정을 이용하여, DC 펄스 마그네트론 스퍼터링 방법에 의해 증착되었다. 시드막은 다양한 Ar/O₂ 압력비에서 증착되었으며, 벌크막은 순수한 Ar가스를 사용하여 증착되었다. 시드막 증착시 산소 압력이 증가함에 따라, 결정성과 (002) 배향성의 정도는 증가했다. 비저항은 시드가 없는 샘플의 경우 $4.7 \times 10^{-4} \Omega \cdot \text{cm}$ 로부터 Ar/O₂ = 9/1 샘플의 경우 $3.7 \times 10^{-4} \Omega \cdot \text{cm}$ 까지, 결정성의 증가와 함께 점차 감소했다. 에칭된 표면은 분화구 형상의 구조를 보여주었으며, 급격한 형상 변화가 결정성 증가와 함께 나타났다. Ar/O₂ = 9/1 조건의 샘플은 500 nm에서 88%의 매우 높은 haze 수치를 보여주었으며, 이는 AFM 이미지에서 보여지는 것처럼 큰 표면 구조 크기에 의해 설명된다.

주제어 : ZnO:Al 박막, 투명전극, 결정성, Si 박막 태양전지

* [전자우편] taeho@lge.com

† [전자우편] hmlee@lge.com